Organic & Biomolecular Chemistry

PAPER

View Article Online
View Journal

Cite this: DOI: 10.1039/c6ob01991a

Catalytic enantioselective acyl transfer: the case for 4-PPY with a C-3 carboxamide peptide auxiliary based on synthesis and modelling studies†

Rudy E. Cozett,[a] Gerhard A. Venter,[a,b] Maheswara Rao Gokada[a] and Roger Hunter*[a]

Received 9th September 2016,
Accepted 28th October 2016

DOI: 10.1039/c6ob01991a

www.rsc.org/obc

A series of 4-pyrrolidinopyridine (4-PPY) C-3 carboxamides containing peptide-based side chains have been synthesised and evaluated in the kinetic resolution of a small library of chiral benzylic secondary alcohols. A key design element was the incorporation of a tryptophan residue in the peptide side chain for promoting π-stacking between peptide side chain and the pyridinium ring of the *N*-acyl intermediate, in which modelling was used as a structure-based guiding tool. Together, a catalyst containing a LeuTrp-*N*-Boc side chain (catalyst **8**) was identified that achieved *s*-values up to and in slight excess of 10. A transition-state model based on the modelling is proposed to explain the origin of enantioselectivity. This study establishes the usefulness of modelling as a structure-based guiding tool for enantioselectivity optimization as well as the potential for developing scalable peptide-based DMAP-type catalysts for large-scale resolution work.

Introduction

The use of chiral 4-dimethylaminopyridine (DMAP) derivatives in the kinetic resolution (KR) of racemic secondary alcohols *via* Lewis-base catalysis has gained considerable momentum since the first example by Vedejs and Chen reported twenty years ago using an asymmetric centre attached to the α-carbon at C-2 of the pyridine ring.[1] Although they achieved high *s*-values (>10), catalyst reactivity was low, with reactions requiring both a Lewis acid and a stoichiometric amount of catalyst for full conversion that was attributed to steric congestion at the "*ortho*" position in accordance with earlier findings by Russian and German investigators.[2] Since then,[3] chiral DMAP-based methodology has blossomed to using the full gamut of chirality types from central,[4] axial[5] to planar.[6]

In more recent work, Seidel[7] has elegantly demonstrated that a suitable chiral environment can be generated using achiral DMAP in conjunction with a chiral thiourea anion binder to bring about the kinetic resolution of amines *via* a chiral ion-pair,[8] resulting in excellent *s*-values. Other types of catalyst for alcohol resolution that have been developed include amidines and bicyclic imidazoles,[9] phosphorus-based,[10] N-heterocyclic carbenes[11] and vicinal diamines,[12] which have all been extensively covered in some excellent recent reviews.[3,13] Recently, 4-PPY KR has been demonstrated to have application to a medicinal chemistry scale-up of an enriched tetrazole hemiaminal ester prodrug for clinical evaluation, in which interestingly Connon's[4g] simple monamide at the 3-position turned out to be the best transfer catalyst.[14]

Peptide catalysts have also been impressively demonstrated, first by Miller,[15] and later by Schreiner[16] and others,[17] using an *N*-methyl histidine residue as the Lewis base to afford high *s*-values in the KR of secondary alcohols, although these types of peptide catalysts are not easily accessed in large amounts. Moreover, and in the context of the present study, to date only two studies[18] have appeared regarding developing a peptide auxiliary (as opposed to mono-amides[4g,19]) in conjunction with a DMAP (or 4-PPY) template in the KR of secondary alcohols, one of them involving a tryptophan residue.[18b] The lack of examples is probably due to the challenge involved of predictively engineering an appropriate interaction between peptide auxiliary and template so as to create a suitable chiral environment around the *N*-acylation centre. However, such a catalyst system would have the obvious advantage over other reported catalysts of being able to produce large quantities of either catalyst enantiomer (as well as diastereomers) for scale-up studies. Furthermore, in spite of the advances made in the field, generally there have been few mechanistic

[a]Department of Chemistry, University of Cape Town, Rondebosch, 7701, South Africa. E-mail: Roger.Hunter@uct.ac.za; Fax: +27 21 6505195; Tel: +27 21 650 2544
[b]Scientific Computing Research Unit, University of Cape Town, Rondebosch, 7701, South Africa

†Electronic supplementary information (ESI) available: A full Experimental section, spectroscopic data of catalysts, HPLC data for the kinetic resolutions and molecular modelling results. See DOI: 10.1039/c6ob01991a

studies,[4a,g,5f,20] regarding the origin of enantioselectivity with DMAP-based catalysts. In this communication we report on the use of molecular modelling as a directing tool in the development of a scalable 4-PPY 3-carboxamide catalyst. The successful catalyst was used in the kinetic resolution of a small library of secondary alcohols, in which strong evidence for π-stacking[20a] of a tryptophan residue with the *N*-acylpyridinium intermediate was obtained.

Results and discussion

Our design strategy was inspired by the work of Fuji and Kawabata,[4a,b] and Yamada.[4c,i] Both authors demonstrated interesting stacking interactions in the *N*-acylpyridinium ion intermediate in order to achieve appropriate pyridine ring facial discrimination. In Fuji's case this was achieved *via* naphthyl-pyridinium π–π stacking, while Yamada's case was postulated to involve a pyridinium-thiocarbonyl group cation-π interaction. In our case it was hoped to invoke a π-stacking interaction involving the π-excessive indole ring of a tryptophan residue in the peptide chain interacting with the electron-deficient *N*-acylpyridinium ion intermediate **1**, Scheme 1.

The first two derivatives targeted were the 4-PPY 3-carboxamides **3** and **4** with Trp and LeuTrp peptide side-chains, respectively (Scheme 2). The idea of introducing Leu as the first amino acid at the carboxyl attachment point was twofold as: (i) to improve dichloromethane (DCM) solubility in the kinetic resolution, and (ii) to possibly provide some screw for discrimination of one of the pyridine faces. Modelling later on vindicated this notion. A 4-pyrrolidino substituent rather than its dimethylamino counterpart facilitated an improved solubility of the catalyst in DCM, the solvent of choice for the kinetic resolutions. Synthesis of **3** and **4** was relatively straightforward based on methodology used by Yamada,[4i] first involving S_NAr of commercially available 4-chloronicotinic acid with pyrrolidine and isolation of the product as its potassium salt **2** in a 95% isolated yield. The latter was then coupled in a pyridine/water mix using EDC and HOBt with either Trp-OMe or Leu-Trp-OMe in yields of around 45% in each case. The Leu-Trp-OMe was prepared by conventional means using an FMoc protecting group for the intermediate and also *via* an EDC coupling, Scheme 2. Yields for the coupling weren't optimized further, but this is likely to be possible on any scale-up. EDC coupling in the 4-PPY derivative synthesis proved to give superior yields compared to those using acid chloride methodology (~25% yield).

The derivatives **3** and **4** were fully characterised by NMR spectroscopies, IR spectroscopy and HRMS. Chiral HPLC of **4** revealed a single peak, which, coupled with a single set of resonances in its ^{13}C NMR spectrum, was taken as sufficient evidence that epimerisation had not taken place. Resolution of 1-(2-naphthyl)ethanol under the standard resolution conditions of 1 equivalent of racemic alcohol, isobutyric anhydride (0.7 eq.) and catalyst (5 mol%), with triethylamine (0.9 eq.) in DCM at −78 °C, led to a decent conversion with each of the catalysts, depending on the substrate, of between 30–60% after three hours, revealing a high acyl-transfer activity of the DMAP derivative. Following chromatographic separation, the usual procedure according to the method of Kagan,[21] of measuring the ees of the product ester and residual alcohol using chiral HPLC resulted in *s*-values of 2.3 (*C* = 42%) for catalyst **3** and an encouraging 5.3 (*C* = 34%) for catalyst **4**. No reaction was observed using triethylamine in the absence of catalyst, in accordance with other studies. Encouraged by the result for **4**, it was decided to use it in a broader substrate study, results of which are shown in Table 1.

The *s*-values were generally low (1.3–3.3), apart from the naphthyl alcohol in entry 1 (5.3), so it was decided to proceed to computer modelling of the *N*-acyl intermediate ($\mathbf{4_{N\text{-}Ac}}$) in

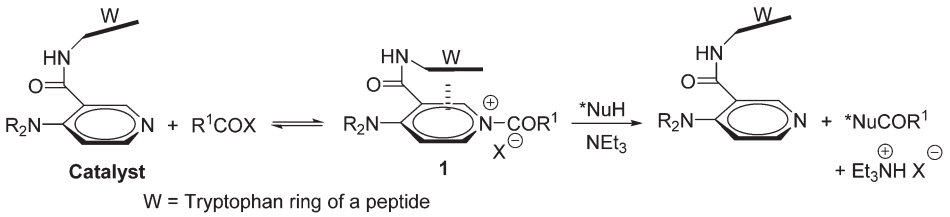

Scheme 1 π-Stacking model for a DMAP-peptide acylation transfer catalyst.

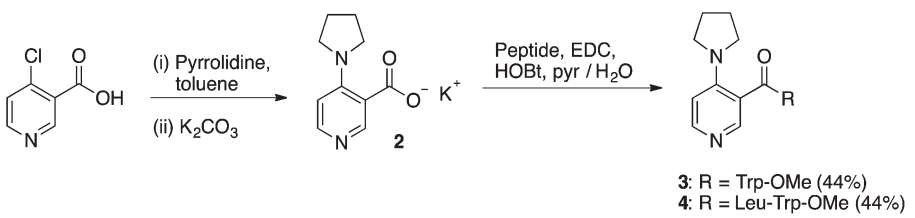

Scheme 2 Synthesis of peptide-PPY catalysts **3** and **4**.

Table 1 The kinetic resolution of various racemic *sec*-alcohols catalysed by **4**

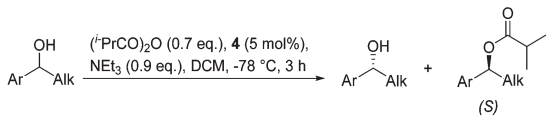

Entry	Substrate	C^a	ee^b alcohol	ee^c ester	s^d	Configuration^e
1	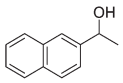	34	31.1	59.4	5.3	(*S*)
2		49	38.6	40.1	3.3	(*S*)
3	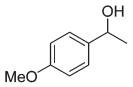	4	21.9	30.3	2.3	(*S*)
4	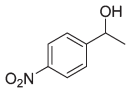	63	12.4	7.1	1.3	(*S*)
5	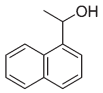	60	48.4	32.2	3.0	(*S*)
6	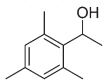	27	17.3	46.3	3.2	(*S*)

^{a} Conversion $C = 100 \times$ (ee of recovered alcohol)/(ee of recovered alcohol + ee of ester). ^{b} ee of recovered alcohol as measured by chiral HPLC on an AD, OD, or IC column. ^{c} ee of the hydrolysed ester (2 M NaOH in MeOH/H_2O as measured on AD, OD, or IC column). ^{d} Selectivity factor $s = \frac{\ln(1-C)(1-\mathrm{ee})}{\ln(1-C)(1+\mathrm{ee})}$ where ee refers to the recovered alcohol. ^{e} The absolute configuration of the faster-reacting enantiomer (ester) and determined by a comparison of $[\alpha]_D^{20}$ values with those reported in the literature.

order to identify potential structural elements for improvement (Fig. 1).

For this purpose, an initial set of 1000 diverse conformers of $\mathbf{4_{N\text{-}Ac}}$, based on a root-mean-square deviation (RMSD) criterion to assure effective spanning of conformational space, was first generated using the Open Babel toolkit,[22] which employs a genetic algorithm for this task. The structure of each conformer was optimized using molecular mechanics and the MMFF94 force field.[23] A subset of the 100 lowest energy conformers was then extracted and further optimized using the efficient HF-3c method.[24] This is a quantum mechanical calculation with three empirical corrections that, aside from corrections for basis set inefficiencies, also includes a dispersion correction. The latter was considered to be important in context, given the role that dispersion interactions were expected to play in stabilising the active conformer of the catalyst. The HF-3c method was developed by Grimme, which is intended for pre-screening applications of large molecules.[24] Subsequently, from these 100 structures, the ten with the lowest energy were further refined using density functional theory (DFT), in which the B3LYP[25–27] hybrid functional and def2–SVP[28] basis set was used in the calculations. In the DFT calculations, dispersion was taken into account by using the well-established D3 dispersion correction of Grimme, with Becke–Johnson damping to assure the correct asymptotic behaviour.[29,30] To speed up these calculations, the resolution of identity (RI) approximation was used to approximate Coulomb integrals[31] as well as a chain of states method for numerical integration of the exchange contribution to the hybrid functional.[32] Finally, since the dipeptides are charged, a further correction was made for solvent stabilization effects during the geometry optimizations, using the conductor-like screening polarizable continuum model (COSMO) with DCM.[33] To further limit computational effort, the effect of an explicitly included anion on the structures, was not taken into account. This level of QM theory is given the shorthand B3LYP–D3(BJ)/def2–SVP. All DFT geometry optimizations were performed with tight convergence criteria and the lowest energy structures were confirmed as minima by the absence of imaginary frequencies in the calculated vibrational spectrum. The vibrational spectra were calculated numerically using two-

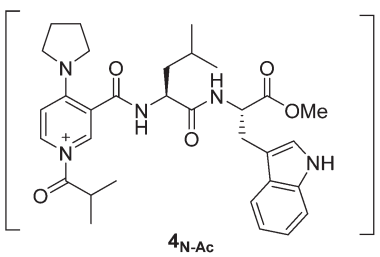

$\mathbf{4_{N\text{-}Ac}}$

Fig. 1 *N*-Acyl-pyridinium cation $\mathbf{4_{N\text{-}Ac}}$ of catalyst **4**.

sided (central) differences with a step size of 0.001 Bohr and it was assumed that imaginary frequencies up to 50 cm^{-1} were due to numerical errors and thus not indicative of a saddle point. The ORCA 3.0.2 software package was used for the quantum mechanical calculations.[34]

Fig. 2 shows the resultant lowest energy conformer, while the full set of ten conformers are given in the ESI.† Based on a Boltzmann distribution of the energies at 298.15 K, the lowest energy conformer had a weight of 90%.

Several points of the conformational analysis deserve mentioning:

• The *N*-acylpyridinium moiety adopts an *s-trans* conformation [τ(C-2^{pyri}, N-1^{pyri}, C^{N-acyl}, O^{N-acyl}) = −172.2°] in which the carbonyl oxygen points away from the more substituted pyridine C-3 side, even though this results in the bulky isopropyl group being brought closer to the C-3 chain. While it may seem counterintuitive that the bulky iso-propyl group is on the same side as the peptide substituent at C-3, this is in agreement with reports by Spivey[5b] and Connon.[4g] Spivey has suggested that while the preferred orientation of the *N*-acyl group is not sterically driven, the orientation of the iso-propyl group may be due to a stereoelectronic stabilisation due to partial conjugation with the C-3 substituent.[5b] We tested this by also performing a geometry optimization of the analogous *s-cis* conformer. The resultant structure had τ(C-2^{pyri}, N-1^{pyri}, C^{N-acyl}, O^{N-acyl}) = −8.6°, but was 41.4 kJ mol^{-1} higher in energy than the minimum (and we return to this point again when discussing compound $\mathbf{8_{N\text{-}Ac}}$).

• The peptide chain curves underneath the pyridinium ring – defined as one looks at it with the C-3 substituent on the right-hand side. This would imply exclusive attack of the incoming secondary alcohol from "the top" or *re* face of the acyl carbonyl group in this case.

• The screw of the chain results in the indole ring being brought close to the acyl site, effectively blocking the *si* (underneath) face of the *N*-acyl carbonyl group. Here, a hydrogen bond can be seen between the indole NH and the first carbonyl group oxygen in the C-3 chain (due to Leu) at a distance of 2.335 Å and an angle of 118.1° – see the left-hand drawing in Fig. 2 – supporting the possibility of an interaction between the indole and the pyridinium ring as originally postulated. The distance between the centroids of the pyridinium and indole benzene ring is 4.435 Å, which is beyond the 3.3–3.8 Å range suggested by Janiack for qualifying as π-stacking.[35] Likewise, the angle between the benzene ring normal and the vector between the centroids, describing the parallel displacement, is approximately 48°. This latter value is again much greater than the 25° found in an ideal gas phase optimized π-stacked benzene-pyridine complex that has a parallel displaced geometry.[36]

Although this therefore does not suggest a substantial stabilizing interaction, it was felt that things were moving in the right direction in that, as shown by the right-hand frame of Fig. 2, H-2 of the pyridinium ring (shown in cyan) lies over the pyrrole ring (shown in magenta) of the indole ring.

Further evidence for the interaction suggested from the modelling was sought from ^{1}H NMR studies. Here, the aim was to study NMR shift differences between the H-2, H-5 and H-6 resonances for **4** and its pyridinium-ion $\mathbf{4_{N\text{-}Me}}$ in the hope of finding evidence for such an interaction. *N*-Methylation[4g] rather than acylation[4a] turned out to be more appropriate in terms of sample handling. As a reference for $\mathbf{4}$/$\mathbf{4_{N\text{-}Me}}$ it was decided to replace the Trp amino acid of the peptide chain with a Leu, so Leu-Leu-OMe was prepared *via* an EDC coupling as before, which in turn was coupled with the 4-PPY nicotinate potassium salt **2**, also using EDC and in pyridine/water as before, affording the dipeptide Leu-Leu catalyst **5** in 27% yield after chromatography ultimately. In turn, both dipeptides were methylated to completion (TLC) with methyl iodide at room temperature in DCM to produce methylated derivatives that were isolated by filtration in the case of $\mathbf{5_{N\text{-}Me}}$ and evaporated directly in the case of $\mathbf{4_{N\text{-}Me}}$. Spectroscopic characterisation (see ESI†) revealed a new *N*-methyl singlet for 3H at δ 3.79 ppm in the ^{1}H NMR spectra of $\mathbf{4_{N\text{-}Me}}$ and one at 4.06 ppm for the $\mathbf{5_{N\text{-}Me}}$ sample confirming that methylation had taken place in each case. The chemical shifts for the three pyridine ring hydrogens in the ^{1}H NMR spectra of each of **4** and **5** were each identified, together with those of their methylated derivatives, based on chemical shift and coupling constant considerations as well as a COSY spectrum for $\mathbf{4_{N\text{-}Me}}$. The chemical shift difference between each corresponding hydrogen of the pyridine ring (H-2, H-5, and H-6) in unmethylated catalysts **4** (Leu-Trp) and **5** (Leu-Leu) was measured as

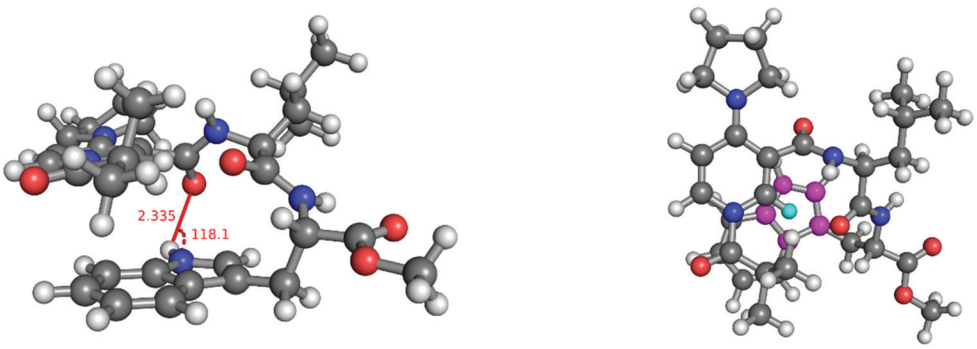

Fig. 2 Two different views of the lowest energy conformer of $\mathbf{4_{N\text{-}Ac}}$.

$\Delta\delta$ ($\delta_5 - \delta_4$), and similarly $\Delta\delta_M$ ($\delta_{5_{N\text{-}Me}} - \delta_{4_{N\text{-}Me}}$) for the methylated derivatives $\mathbf{4_{N\text{-}Me}}$ and $\mathbf{5_{N\text{-}Me}}$. The results are shown in Table 2.

The results were indeed very informative. Comparing all three individual pyridine resonances for **4** and **5** revealed a 0.014 ppm downfield shift ($\Delta\delta$) for H-2 going from **4** to **5**, and virtually no changes for H-5 and H-6 ($\Delta\delta \sim 0$). Turning to the data for the salts, however, gave a much different picture. While both H-2 resonances for $\mathbf{4_{N\text{-}Me}}$ and $\mathbf{5_{N\text{-}Me}}$ were deshielded relative to those for their neutral counterparts **4** and **5** (0.15 ppm for the **4** series and 0.61 ppm for the **5**), the H-6 resonances for the salts were actually shielded compared to those for **4** and **5** (0.47 ppm for the **4** series and 0.37 ppm for the **5**). Understandably, in view of proximity as well as resonance and inductive considerations, H-5 was far less responsive and was only slightly deshielded going from neutral compound to salt (0.08 ppm in the **4** series and 0.19 ppm in the **5**). While the shielding of H-6 going from **5** to $\mathbf{5_{N\text{-}Me}}$ (8.14 ppm to 7.77 ppm) was surprising, the most striking relationship emerging from the data in the context of the modelling results was the relatively large difference between the chemical shifts of H-2 in the salts ($\Delta\delta_M$ = 0.60). Comparing with the fairly negligible $\Delta\delta_M$ values for H-5 and H-6 revealed a significant shielding of H-2 in the LeuTrp salt $\mathbf{4_{N\text{-}Me}}$, in agreement with the modelling image in Fig. 2 showing a π-stacking-type interaction between H-2 (cyan) and the pyrrole ring of the tryptophan indole ring. Further support was obtained from a NOESY experiment, which showed a correlation between H-2 and the indole NH and an adjacent hydrogen (α to NH as H-5 or on the A-ring H-10 – see the ESI† for numbering) as well as to NH_{Trp}. Weaker correlations were identified between the pyridine H-5 and H-6 hydrogens and the indole A-ring hydrogens. Taken together this suggests a stacking-type interaction in which H-2 comes closest (of the three pyridine ring protons) to the indole ring shielding zone. Furthermore, a COSY spectrum of $\mathbf{4_{N\text{-}Me}}$ revealed the NH_{Leu} hydrogen (of the first peptide of the chain) to be significantly deshielded compared to that in **4** (6.73 to 8.78 ppm). The deshielding indicates an increase in the δ^+ character of the H of NH_{Leu}, which in turn implies a greater delocalisation of the N lone pair into the carbonyl, presumably to compensate for the electron-withdrawing effect of the adjacent pyridinium ring. Such an increase in δ^- character at the first carbonyl oxygen would be consistent with the important hydrogen bond between the indole NH and the first carbonyl oxygen of the chain as identified by the modelling in Fig. 2. While the NMR and modelling views have subtle differences regarding indole and pyridinium ring alignment, taken together these results provide compelling support for a significant interaction between the π-deficient pyridinium and π-excessive indole ring as indicated in Fig. 2, and in line with modern thinking on the structural requirements required to promote enantioselectivity in chiral DMAP Lewis base catalysis.

Based on these conclusions, in the next phase of the project it was decided to extend the peptide chain from dipeptide to tripeptide retaining the indole in the middle position. This was intended to explore whether extra length in the chain might help with buttressing on the C-5/C-6 side ("left-hand" side). The terminal residue was chosen as either Leu or Trp, syntheses of which are shown in Schemes 3 and 4. For the Leu-Trp-Trp catalyst **6** a Boc protecting group was used throughout the peptide coupling sequence, and coupling the tripeptide Leu-Trp-Trp-OMe to the 4-PPY nicotinate salt **2** in a pyr/H_2O mix and EDC as before, furnished a 53% yield of **6**. Conversely, for the Leu-Trp-Leu catalyst a combination of Boc and FMoc protecting groups was utilised in which the final coupling to afford the actual catalyst **7** was 44%. Spectroscopic data, notably the single set of resonances in the ^{13}C NMR spectra, suggested a single diastereomer for each catalyst, which was supported by chiral HPLC data for **7**, which revealed a >98% purity as a single enantiomer and diastereomer.

Kinetic resolution experiments were then carried out as before and the results are shown in Table 3 for tripeptide catalysts **6** and **7**:

Unfortunately, the *s*-values for tripeptide catalysts **6** and **7** showed lower selectivity than those of the dipeptide catalyst **4**. Additionally, the Leu-Trp-Leu catalyst **7** showed much slower conversion so was only tested against the naphthyl substrate (entry 5 in Table 3), which gave C = 5.8% at −78 °C for 3 h; s = 3.3, and for which the LeuTrp dipeptide **4** had given the best result of s = 5.3 at around 50% conversion. A longer time of 12 h with **7** (entry 6) did raise the conversion to an acceptable level (46%), but the *s*-value dropped to 2.4. Similarly, the addition of a Trp residue to the dipeptide terminus of **4** diminished resolution efficiency (catalyst **6**, entries 1–4), possibly by presenting competing conformational options with conflicting resolution outcomes. The possibility of the intermediacy of peptide aggregates also can't be discounted in this case in view of the significant lowering in reaction rate. In any event,

Table 2 ^1H NMR chemical shifts (ppm) of the pyridine hydrogens for **4**, **5**, and their methylated analogues

$\mathbf{4_{N\text{-}Me}}$ and $\mathbf{5_{N\text{-}Me}}$

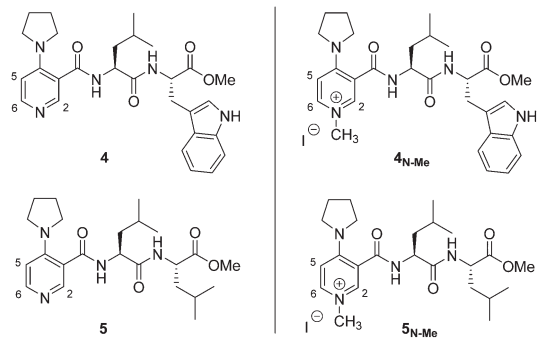

$H^{a,b}$	δ**4**	δ**5**	$\Delta\delta^c$	$\delta\mathbf{4_{N\text{-}Me}}$	$\delta\mathbf{5_{N\text{-}Me}}$	$\Delta\delta_M$ [d]
H-2	8.12	8.26	0.14	**8.27**	**8.87**	**0.60**
H-5	6.43	6.47	0.04	6.51	6.66	0.15
H-6	8.14	8.14	0.0	7.67	7.77	0.10

[a] $CDCl_3$ as solvent. [b] All pyridine resonances were unambiguously assigned by NMR spectroscopy (^1H, and COSY). [c] The $\Delta\delta$ value for each resonance corresponds to $\delta_5 - \delta_4$. [d] The $\Delta\delta_M$ values correspond to $\delta_{5_{N\text{-}Me}} - \delta_{4_{N\text{-}Me}}$ for the methylated series.

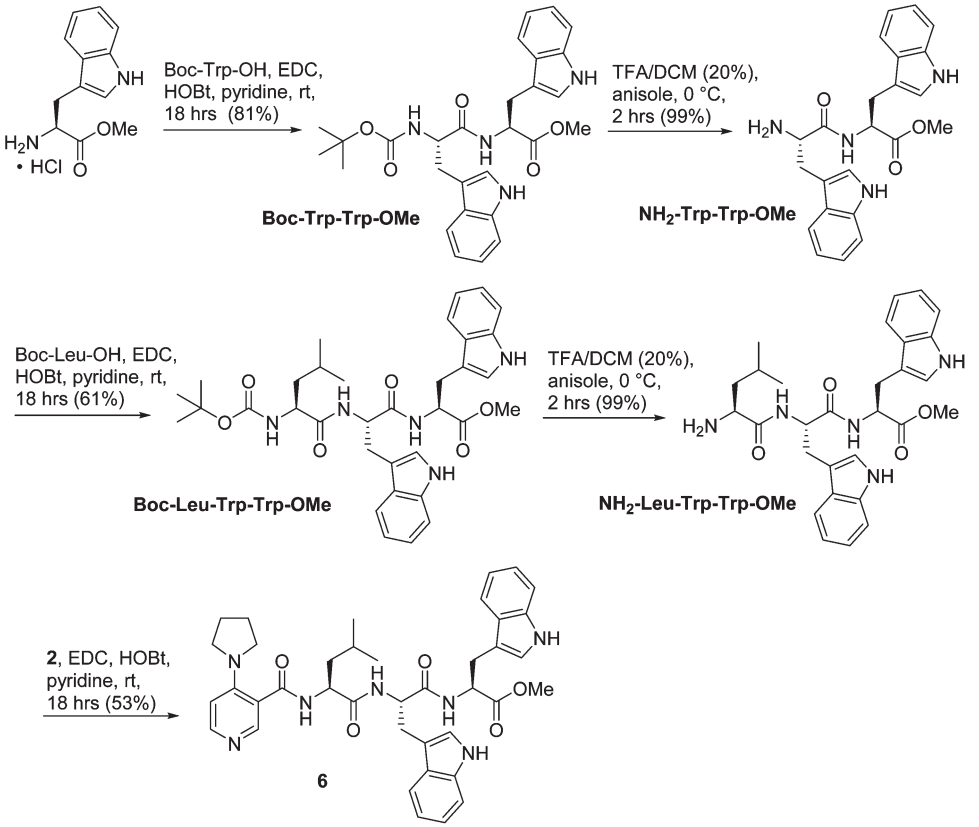

Scheme 3 Synthesis of Leu-Trp-Trp tripeptide catalyst **6**.

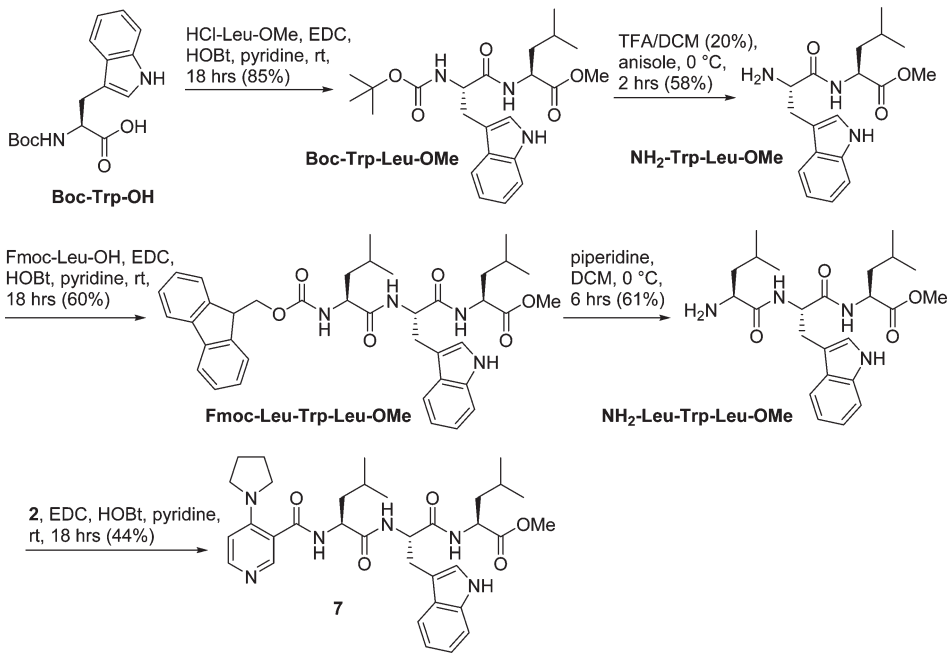

Scheme 4 Synthesis of Leu-Trp-Leu tripeptide catalyst **7**.

Table 3 The kinetic resolution of various racemic *sec*-alcohols catalysed by **6** or **7**

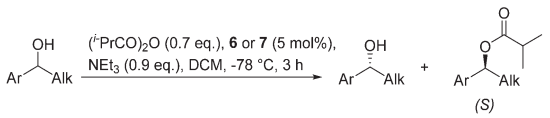

Entry[a]	Catalyst	Substrate	*C*	ee[b] alcohol	ee[c] ester	*s*[d]	Configuration[e]
1	**6**		28	10.7	28.2	2.0	(*S*)
2	**6**	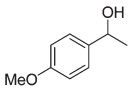	35	12.1	22.3	1.8	(*S*)
3	**6**	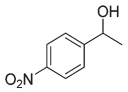	53	7.6	6.7	1.2	(*S*)
4	**6**	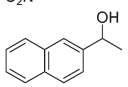	51	21.6	21.1	1.9	(*S*)
5	**7**	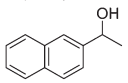	5.8	3.2	52.5	3.3	(*S*)
6	**7**	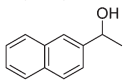	46[f]	26.4	30.4	2.4	(*S*)

[a] Conditions = alcohol (1.0 eq.), cat (5 mol%), (i-PrCO)$_2$O (0.7 eq.), NEt$_3$ (0.9 eq.), −78 °C, DCM, 3 h. [b] ee of recovered alcohol as measured by chiral HPLC on a AD, OD, or IC column. [c] ee of the hydrolysed ester (2 M NaOH in MeOH/H$_2$O as measured on a AD, OD, or IC column). [d] Selectivity factor $s = \frac{\ln(1-C)(1-\mathrm{ee})}{\ln(1-C)(1+\mathrm{ee})}$ where ee refers to the recovered alcohol. [e] The absolute configuration of the faster-reacting enantiomer (ester) and determined by a comparison of $[\alpha]_D^{20}$ values with those reported in the literature. [f] T = 12 h.

"bigger isn't always better" seemed to be the message so we returned to modelling for scientific direction. Modelling of the *N*-acylpyridinium ion of Leu-Trp dipeptide **4** (Fig. 2) suggested that C-6 and C-7 of the indole A-ring could be fruitful avenues of functionalization to pursue in order of the possibility of providing extra buttressing, but this would require a new and more complex synthesis. Hence, as a second choice of pursuit it was decided to remove the hydrogen bond shown in Fig. 2, and *N*-protect in which a Boc protection was chosen in view of its likely ease of introduction as well as the steric bulk of the *t*-butyl group (catalyst **8**).

To gain further insight into the possible consequence of this choice, the calculation procedure outlined before was again repeated to produce ten low-energy conformers of $\mathbf{8_{N\text{-}Ac}}$. Fig. 3 shows the resultant lowest energy conformer, again with the full set of ten conformers given in the ESI.† Based on a Boltzmann distribution of the energies at 298.15 K, the lowest energy conformer of $\mathbf{8_{N\text{-}Ac}}$ had a weight of 97%.

Gratifyingly, these calculations presented a more promising conformational picture for improving the *s*-factor with salient features as follows:

• As with the LeuTrp-NH catalyst **4** ($\mathbf{4_{N\text{-}Ac}}$), the dipeptide chain of **8** ($\mathbf{8_{N\text{-}Ac}}$) coils underneath the pyridinium ring, with the C-3 substituent on the "right". However, the *N*-acyl group is now in an *s-cis* conformation with τ(C-2$^{\mathrm{pyri}}$, N-1$^{\mathrm{pyri}}$, C$^{\mathrm{N-acyl}}$, O$^{\mathrm{N-acyl}}$) = −14.8°. Further calculations showed that this is indeed the most favourable orientation, with the *s-trans* conformer, τ(C-2$^{\mathrm{pyri}}$, N-1$^{\mathrm{pyri}}$, C$^{\mathrm{N-acyl}}$, O$^{\mathrm{N-acyl}}$) = 179.0°, 14.0 kJ mol^{-1} higher in energy. Apart from the configurational reversal, it is interesting to note that the difference in energy between the two conformations is much lower in $\mathbf{8_{N\text{-}Ac}}$ (14.0 kJ mol^{-1}) than that in $\mathbf{4_{N\text{-}Ac}}$ (41.4 kJ mol^{-1}). Comparison of the two structures shows, in the case of $\mathbf{8_{N\text{-}Ac}}$, that the conformation switch can be related to a change in coordinates that is restricted mainly to the *N*-acyl group, whereas for $\mathbf{4_{N\text{-}Ac}}$ there are several additional changes in the relative coordinates of other atoms (*i.e.* in the peptide chain), not directly involved in the torsional change. This leads to the loss of a number of stabilizing intramolecular interactions when the conformation of $\mathbf{4_{N\text{-}Ac}}$ changes from *s-trans* to *s-cis*. Specifically, the greater driving force for structural change in the $\mathbf{4_{N\text{-}Ac}}$ case could be primarily due to the close approach of the 2$^{\mathrm{nd}}$ carbonyl group oxygen (Leu) of the peptide chain to the oxygen atom of the twisted *N*-acyl group in $\mathbf{4_{N\text{-}Ac}}$ *s-cis*, the $O_{\mathrm{N-acyl}}\cdots O_{\mathrm{peptide}}$ distance being 4.24 Å. Other changes include an adjustment in the relative orientation of the indole ring, the loss of intramolecular interaction between this carbonyl group and the C-2 hydrogen atom of the pyridinium ring as well as the absence of the hydrogen bond between the indole NH and the first carbonyl group oxygen, already mentioned earlier (see the ESI† for further details of how these interactions were identified and can be illustrated). Conversely, in $\mathbf{8_{N\text{-}Ac}}$ *s-cis*, the corresponding $O_{\mathrm{N-acyl}}\cdots O_{\mathrm{peptide}}$ distance is 7.28 Å, due to the different orientation of the 2$^{\mathrm{nd}}$ carbonyl group that points away from the

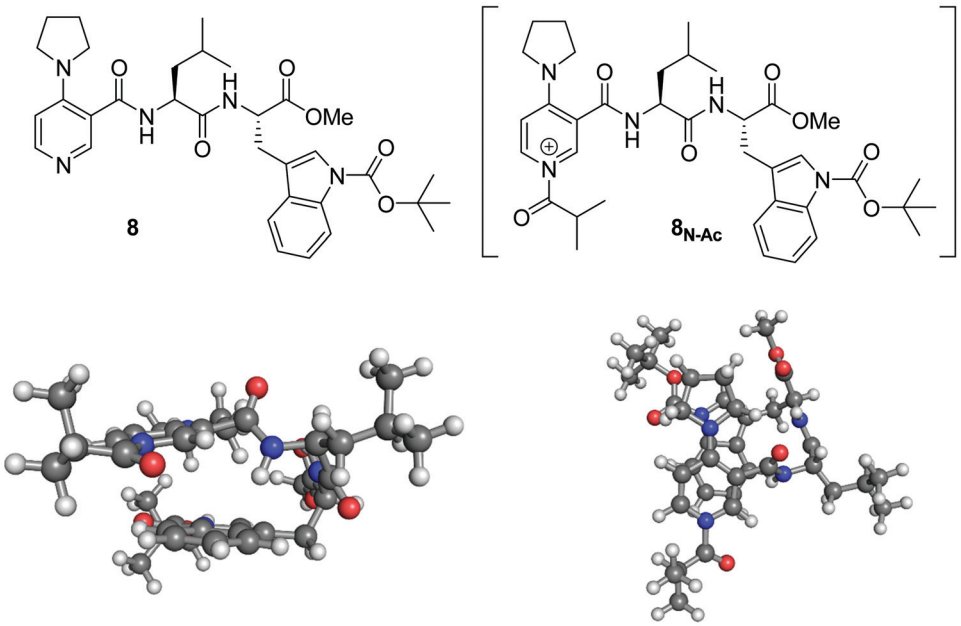

Fig. 3 Two different views of the lowest energy conformer of $\mathbf{8}_{\mathbf{N\text{-}Ac}}$.

N-acyl group, which obviates the need for any further adjustments as the conformation changes.

• The first carbonyl group of the side chain of $\mathbf{8}_{\mathbf{N\text{-}Ac}}$ had a dihedral angle τ(C-2^{pyri}, C-3^{pyri}, C, O) = −120.5°. While not perpendicular to the plane of the pyridine ring exactly, the C=O group effectively points "up" compared to "down" for that of $\mathbf{4}_{\mathbf{N\text{-}Ac}}$, the latter due to hydrogen bonding. This result was deemed to have great significance later.

• Boc introduction into the dipeptide results in a shift of the indole ring to lie more associated with ("underneath") the pyridinium ring of $\mathbf{8}_{\mathbf{N\text{-}Ac}}$ (see Fig. 3, right-hand frame), consequently also minimising steric strain between the pyrrolidino group and the Boc *t*-butyl group. The distance between the centroids of the pyridinium and indole benzene ring is 3.734 Å, and the angle between the benzene ring normal and the vector between the centroids, approximately 30°. In this regard, one can now consider this to show an improved degree of π-stacking.[34] However, the Boc group points "north" away from C-4 rather than emerging on the C-5/C-6 pyridine ring side where buttressing with the substrate might occur.

Encouraged by these results, *N*-Boc dipeptide catalyst **8** was synthesised by reacting **4** with di-*tert*-butyl dicarbonate (3 eq.) in THF at 20 °C to minimise the risk of any epimerisation. Following a basic work-up, the crude product was purified by column chromatography using 10% MeOH/DCM, and catalyst **8** was isolated in a 89% yield as a pale-yellow solid, Scheme 5.

The structure of catalyst **8** was unequivocally assigned on the basis of its spectroscopic data using a combination of 1D, 2D ^{1}H and ^{13}C NMR as well as IR and high resolution mass spectrometry. Importantly, a single set of resonances was observed in both spectra with no sign of any diastereomers. A new upfield singlet in the ^{1}H NMR spectrum present at δ_H 1.64 integrating for nine protons confirmed the introduction of the Boc group. Two samples were prepared, which by chiral HPLC gave peak areas of 98 and 99% respectively (see the ESI†). This was deemed to be good enough for the resolution experiments, in which the 98% catalyst was used for the bulk results, since this was the one produced in quantity.

As before (Table 1) KR experiments with catalyst **8** were run, this time on an extended library and the results are shown in Table 4, in descending order of *s*-values within any series (single *vs.* double ring substrates):

Introduction of the Boc group significantly enhanced the *s*-values, with three entries (entries 1, 2, and 9) exceeding the

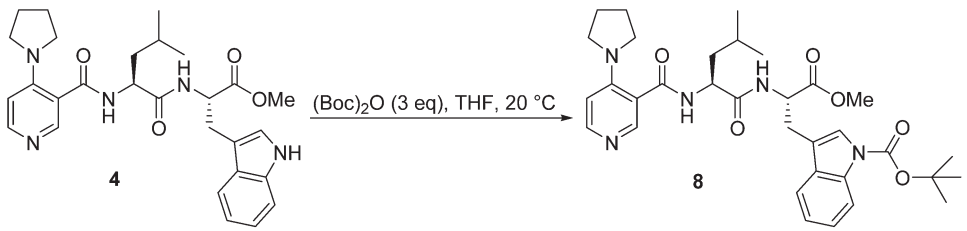

Scheme 5 Synthesis of catalyst **8**.

Table 4 The kinetic resolution of racemic *sec*-alcohols catalysed by **8**

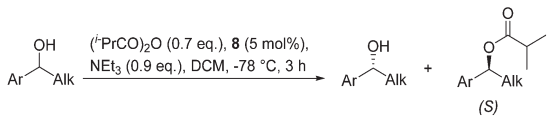

Entry[a]	Substrate	C_{HPLC} [b]	ee (alcohol)[c]	ee (ester)	*s*-Value[d]	Configuration[e]
1	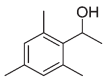	44	57.1	72.0	10.8	(*S*)
2	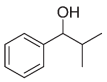	50	68.5	68.8	10.9	(*S*)
3	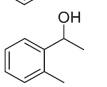	44	53.8	69.9	9.6	(*S*)
4	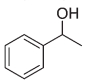	42	50.2	69.1	8.9	(*S*)
5	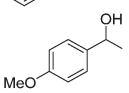	30	29.4	68.0	7.0	(*S*)
6	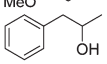	20	16.2	65.3	5.6	(*S*)
7	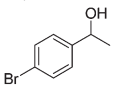	45	35.7	43.1	3.5	(*S*)
8	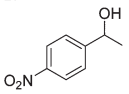	36	13.9	24.6	1.9	(*S*)
9	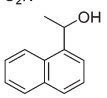	45	59.3	71.1	10.7	(*S*)
10	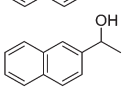	50	63.2	62.4	8.1	(*S*)
11	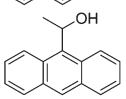	56	50.6	39.8[f]	3.7	(*S*)
12	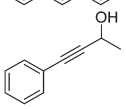	11	3.6	30.6	1.9	(*S*)

[a] Conditions = alcohol (1.0 eq.), cat (5 mol%), (i-PrCO)$_2$O (0.7 eq.), NEt_3 (0.9 eq.), −78 °C, DCM, 3 h. [b] ee of recovered alcohol as measured by chiral HPLC on an AD, OD, or IC column. [c] ee of the hydrolysed ester (2 M NaOH in MeOH/H_2O as measured on an AD, OD, or IC column). [d] Selectivity factor $s = \frac{\ln(1 - C)(1 - \text{ee})}{\ln(1 - C)(1 + \text{ee})}$ where ee refers to the recovered alcohol. [e] The absolute configuration of the faster-reacting enantiomer (ester) and determined by a comparison of $[\alpha]_D^{20}$ values with those reported in the literature. [f] Ester not hydrolysed but measured directly.

synthetically useful benchmark value for *s* of 10. Entries 1–8 show the influence of substitution on the aromatic ring (entries 1, 3, 5, 7 and 8) of 1-phenylethanol or in the chain (entries 2 and 6). Notably, the standard substrate 1-phenylethanol (entry 4) used throughout studies in the literature (entry 4) returned a value of 8.9, almost a threefold improvement compared to that of catalyst **3** without the Boc group (*s* = 3.3, entry 2, Table 1) and one similar or better for chiral DMAP catalysts with DMAP C-3 amide-based auxiliaries. The introduction of a steric effect in the form of methyl groups either on the ring or chain resulted in very good *s*-values around 10 (entries 1–3) with no compromising of the conversion, which stayed close to 50%. By comparison, substitution of the substrate phenyl ring with electron-donating or releasing groups favoured the former rather than the latter (entry 5 with a *p*-OMe, *s* = 7.0 *versus* entry 7 with a *p*-Br, *s* = 3.5 and entry 8 with *p*-NO_2, *s* = 1.9), suggesting the importance of a π-stacking interaction in view of the *s*-value increasing with increasing electron density in the substrate phenyl ring promoting a tighter interaction with the electron-deficient pyridinium ring. Moving the stereogenic centre one down the chain in the form of 1-phenyl-2-propanol returned an encouraging value of 5.6 for an

aliphatic alcohol (entry 6). Similarly, in the naphthalene series, with the chiral hydroxyethyl side-chain at the naphthalene 2-position, the *s*-value rose from 5.3 (entry 1, Table 1) with catalyst **4** to 8.1 (entry 10, Table 4) with **8**. Furthermore, shifting the side-chain to the 1-position resulted in the *s*-value increasing to a respectable value of 10.7. Conversely, extending the same chiral side-chain to the 9-position of anthracene reduced the *s*-value to a low 4.0 probably due to its greater symmetrical nature with a choice of rings for π-stacking, but still with good conversion (54%). This reduction in value continued with propargylic alcohol in entry 12 to a very low 1.9, presumably now to inefficient π-stacking with the triple bond, as suggested by the low conversion (11%) under the same conditions and time. These latter results indicate the relative importance of the electronic effect over the steric one. In all cases, the fast-reacting enantiomer was the *S*-enantiomer as determined by measuring the sign of the optical rotations and comparing them to literature values.

Fig. 4 outlines a possible transition-state model for the two enantiomers of 1-phenylethanol reacting with $\mathbf{8}_{\mathbf{N\text{-}Ac}}$ based on the modelling data. Importantly, π-stacking is postulated to occur between the substrate aromatic ring and the top face of the catalyst pyridine ring, with the *N*-Boc indole moiety blocking the underneath face as suggested by the modelling data (Fig. 4 – only the C═O group of the chain is shown). The minimum energy conformation of the α-hydroxyalkyl substituent containing the stereogenic centre is taken as having the methyl group perpendicular and pointing away from the plane of the pyridine ring in order to minimise allylic strain between the methyl group of the alcohol and the *ortho*-hydrogens of the substrate aryl ring in accordance with Birman and Houk's theoretical findings on Birman's amidine catalyst.[37] These considerations result in transition states I and II for the (*S*)- and (*R*)-enantiomers respectively. Importantly, stereoelectronic alignment between the hydroxyl oxygen and the *N*-acyl carbonyl carbon in TS-I allows for the substrate's aromatic ring to slide away from the leucine carbonyl group pointing "up", placing it over to the left-hand side (pyridine C-5/C-6). This results in the minimisation of steric strain between the phenyl ring and the leucine carbonyl group pointing upwards as shown in TS-I. By comparison, the same considerations applied to TS-II for the (*R*)-enantiomer result in an increase in phenyl/CO steric strain. These findings are in agreement with an argument put forward by Yamada in his thiocarbonyl-based catalysis studies.[4i] They also offer an explanation of why the *s*-value increases significantly going from catalyst **4** to **8**. In the former the carbonyl group is pointing "down" due to H-bonding while the NH is pointing "up" but is further out (Fig. 2).

This model doesn't take into account the likely influence exerted by the counter anion associated with the pyridinium ion in terms of both hydrogen bonding and steric strain.[5f,19b] Though the *s*-values in this study with our best catalyst **8** are only just touching on the synthetically useful benchmark of 10, the modelling data strongly suggests that further progress can be made using this structure-based approach. The question of the intermediacy of peptide aggregates is an obvious transition-state complication that cannot be totally discounted and one that wasn't considered by the modelling. However, the fact that reactions involved clear solutions (DCM) at −78 °C, and were fast compared to other kinetic resolutions with similar catalysts, very likely indicates that reactions with catalyst **8** proceed *via* a monomeric species under the conditions described. All things considered, obvious possibilities for improvement would include: (i) introducing H-bonding effects in the peptide side chain so as to promote a tighter binding between catalyst, substrate and counter-ion to the *N*-acylpyridinium ion as noted by Connon[4g] and Sunoj,[38] as well as (ii) increasing the tightness of the π-stacking by placing appropriate substituents (non-stereogenic) on the indole ring and/or at C-5[5e,39] of the pyridinium ring. Finally, as shown by Spivey,[5e] changing the *N*-pyrrolidino group to a long-chain dialkylamino substituent might also have a favourable effect on the *s*-values.

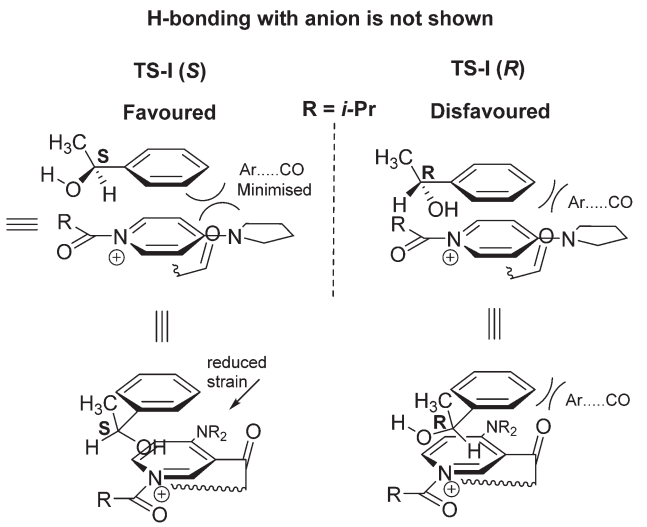

Fig. 4 Proposed transition-state models for the two enantiomers of 1-phenylethanol interacting with *N*-acylpyridinium ion $\mathbf{8}_{\mathbf{N\text{-}Ac}}$.

Conclusions

In conclusion, the results of this study have demonstrated the usefulness of applying rational design principles based on modelling data to developing peptides in a modular way as desirable green, and synthetically stable scalable auxiliaries in chiral DMAP-type Lewis base enantiocatalysis. Such an approach avoids having to use wasteful resolution protocols for catalyst enantiomer synthesis.[5d,6i]

Acknowledgements

We thank the South African National Research Foundation (NRF) for financial support towards this project. Computations were performed using facilities provided by the University of

Cape Town's ICTS High Performance Computing team: http://hpc.uct.ac.za.

References

1 E. Vedejs and X. Chen, *J. Am. Chem. Soc.*, 1996, **118**, 1809–1810.

2 (*a*) G. Höfle, W. Steglich and H. Vorbrüggen, *Angew. Chem., Int. Ed. Engl.*, 1978, **17**, 569–583; (*b*) L. I. Bondarenko, A. I. Kirichenko, L. M. Litvinenko, I. N. Dimitrenko and V. D. Kobets, *Zh. Org. Khim.*, 1981, **17**, 2588–2594.

3 R. P. Wurtz, *Chem. Rev.*, 2007, **107**, 5570–5595.

4 (*a*) T. Kawabata, M. Nagato, K. Takasu and K. Fuji, *J. Am. Chem. Soc.*, 1997, **119**, 3169–3170; (*b*) T. Kawabata, K. Yamamoto, Y. Momose, H. Yoshida, Y. Nagaoka and K. Fuji, *Chem. Commun.*, 2001, 2700–2701; (*c*) S. Yamada, T. Misono and S. Tsuzuki, *J. Am. Chem. Soc.*, 2004, **126**, 9862–9872; (*d*) D. Díez, M. J. Gil, R. F. Moro, N. M. Garrido, I. S. Marcos, P. Basabe, F. Sanz, H. B. Broughton and J. G. Urones, *Tetrahedron: Asymmetry*, 2005, **16**, 2980–2985; (*e*) T. Poisson, M. Penhoat, C. Papamicael, G. Dupas, V. Dalla, F. Marsais and V. Levacher, *Synlett*, 2005, 2285–2288; (*f*) T. Poisson, M. Penhoat, C. Papamicael, G. Dupas, V. Dalla, F. Marsais and V. Levacher, *Synlett*, 2005, 2285–2288; (*g*) C. O. Dálaigh, S. J. Hynes, J. E. O'Brien, T. McCabe, D. J. Maher, G. W. Watson and S. J. Connon, *Org. Biomol. Chem.*, 2006, **4**, 2785–2793; (*h*) H. V. Nguyen, D. C. D. Butler and C. J. Richards, *Org. Lett.*, 2006, **8**, 769–772; (*i*) S. Yamada, T. Misono, Y. Iwai, A. Masumizu and Y. Akiyama, *J. Org. Chem.*, 2006, **71**, 6872–6880.

5 (*a*) A. C. Spivey, P. Charbonneau, T. Fekner, D. H. Hochmuth, A. Maddaford, C. Malardier-Jugroot, A. J. Redgrave and M. A. Whitehead, *J. Org. Chem.*, 2001, **66**, 7394–7401; (*b*) A. C. Spivey, A. Maddaford, D. P. Leese and A. J. Redgrave, *J. Chem. Soc., Perkin Trans. 1*, 2001, 1785–1794; (*c*) K. Jeong, S. Kim, H. Park, K. Chang and K. S. Kim, *Chem. Lett.*, 2002, 1114–1115; (*d*) A. C. Spivey, F. Zhu, M. B. Mitchell, S. G. Davey and R. L. Jarvest, *J. Org. Chem.*, 2003, **68**, 7379–7385; (*e*) A. C. Spivey, D. P. Leese, F. Zhu, S. G. Davey and R. L. Jarvest, *Tetrahedron*, 2004, **60**, 4513–4525; (*f*) E. Larionov, M. Mahesh, A. C. Spivey, A. C. Y. Wei and H. J. Zipse, *J. Am. Chem. Soc.*, 2012, **134**, 9390–9399; (*g*) G. Ma, J. Deng and M. P. Sibi, *Angew. Chem., Int. Ed.*, 2014, **44**, 12012–12015.

6 (*a*) J. C. Ruble and G. C. Fu, *J. Org. Chem.*, 1996, **61**, 7230–7231; (*b*) J. C. Ruble, H. A. Latham and G. C. Fu, *J. Am. Chem. Soc.*, 1997, **119**, 1492–1493; (*c*) J. C. Ruble, J. Tweddell and G. C. Fu, *J. Org. Chem.*, 1998, **63**, 2794–2795; (*d*) C. E. Garrett and G. C. Fu, *J. Am. Chem. Soc.*, 1998, **120**, 7479–7483; (*e*) C. E. Garrett, M. M. Lo and G. C. Fu, *J. Am. Chem. Soc.*, 1998, **120**, 10276–10276; (*f*) B. Tao, J. C. Ruble, D. A. Hoic and G. C. Fu, *J. Am. Chem. Soc.*, 1999, **121**, 5091–5092; (*g*) S. Bellemin-Laponnaz, J. Tweddell, J. C. Ruble, F. M. Breitling and G. C. Fu, *Chem. Commun.*, 2000, 1009–1010; (*h*) J. G. Seitzberg, C. Dissing, I. Sotofte, P. Norrby and M. Johannsen, *J. Org. Chem.*, 2005, **70**, 10890; (*i*) R. P. Wurz, E. C. Lee, J. C. Ruble and G. C. Fu, *Adv. Synth. Catal.*, 2007, **349**, 2345–2352; (*j*) B. Hu, M. Mend, Z. Wang, W. Du, J. S. Fossey, X. Hu and W.-P. Deng, *J. Am. Chem. Soc.*, 2010, **132**, 17041–17044; (*k*) For a helicenoidal chiral DMAP catalyst, see: M. R. Crittall, H. S. Rzepa and D. R. Carbery, *Org. Lett.*, 2011, **13**, 1250–1253 and M. R. Crittall, N. W. G. Fairhurst and D. R. Carbery, *Chem. Commun.*, 2012, **48**, 11181–11183; (*l*) S. Y. Lee, J. M. Murphy, A. Ukai and G. C. Fu, *J. Am. Chem. Soc.*, 2012, **134**, 15149–15153.

7 D. Seidel, *Synlett*, 2014, 783–794.

8 J. Briere, S. Oudeyer, V. Dalla and V. Levacher, *Chem. Soc. Rev.*, 2012, **41**, 1696–1707.

9 (*a*) X. Li, H. Jiang, E. W. Uffman, L. Guo, Y. Zhang, X. Yang and V. B. Birman, *J. Org. Chem.*, 2012, **77**, 1722–1737; (*b*) Z. Zhang, M. Wang, F. Xie, H. Sun and W. Zhang, *Adv. Synth. Catal.*, 2014, **356**, 3164–3170.

10 T. A. Duffey, J. A. MacKay and E. Vedejs, *J. Org. Chem.*, 2010, **75**, 4674–4685.

11 (*a*) Y. Suzuki, K. Yamaguchi, K. Muramatsu and M. Sato, *Chem. Commun.*, 2004, 2770–2771; (*b*) T. Kano, K. Sasaki and K. Maruoka, *Org. Lett.*, 2005, **7**, 1347–1349.

12 (*a*) Y. Kawamata and T. Oriyama, *Chem. Lett.*, 2010, **39**, 382–384; (*b*) E. P. Kündig, A. Enríquez-Garcia, T. Lomberget and G. Bernadinelli, *Angew. Chem., Int. Ed.*, 2006, **118**, 104–107.

13 (*a*) E. Vedejs and M. Jure, *Angew. Chem., Int. Ed.*, 2005, **44**, 3974–4001; (*b*) A. C. Spivey and S. Arseniyadis, *Top. Curr. Chem.*, 2010, **291**, 233–280; (*c*) H. Pellissier, *Adv. Synth. Catal.*, 2011, **353**, 1613–1666; (*d*) C. E. Muller and P. R. Schreiner, *Angew. Chem., Int. Ed.*, 2011, **50**, 6012–6042.

14 D. W. Piotrowski, A. S. Kamlet, A.-M. R. Dechert-Schmitt, J. Yan, T. A. Brandt, J. Xiao, L. Wei and M. T. Barrila, *J. Am. Chem. Soc.*, 2016, **138**, 4818–4823.

15 (*a*) S. J. Miller, G. T. Copeland, N. Papaioannou, T. E. Horstmann and E. M. Ruel, *J. Am. Chem. Soc.*, 1998, **120**, 1629–1630; (*b*) G. T. Copeland, E. R. Jarvo and S. J. Miller, *J. Org. Chem.*, 1998, **63**, 6784–6785; (*c*) E. R. Jarvo, G. T. Copeland, N. Papaioannou, P. J. Bonitatebus and S. J. Miller, *J. Am. Chem. Soc.*, 1999, **121**, 11638–11643; (*d*) M. M. Vasbinder, E. R. Jarvo and S. J. Miller, *Angew. Chem., Int. Ed.*, 2001, **40**, 2824–2827; (*e*) G. T. Copeland and S. J. Miller, *J. Am. Chem. Soc.*, 2001, **123**, 6496–6502; (*f*) M. B. Fierman, D. J. O'Leary, W. E. Steinmetz and S. J. Miller, *J. Am. Chem. Soc.*, 2004, **126**, 6967; (*g*) S. Miller, *Acc. Chem. Res.*, 2004, **37**, 601–610; (*h*) E. A. Colby Davie, S. M. Mennen, Y. Xu and S. J. Miller, *Chem. Rev.*, 2007, **107**, 5759–5812.

16 (*a*) L. Wanka, C. Cabrele, M. Vanejews and P. R. Schreiner, *Eur. J. Org. Chem.*, 2007, 1474–1490; (*b*) C. E. Müller, L. Wanka, K. Jewell and P. R. Schreiner, *Angew. Chem., Int. Ed.*, 2008, **47**, 6180–6183; (*c*) C. E. Müller, D. Zell and P. R. Schreiner, *Chem. – Eur. J.*, 2009, **15**, 9647–9650; (*d*) R. Hrdina, C. E. Müller and P. R. Schreiner, *Chem. Commun.*, 2010, **46**, 2689–2690.

17 (*a*) K. Ishihara, Y. Kosugi and M. Akakura, *J. Am. Chem. Soc.*, 2004, **126**, 12212–12213; (*b*) F. Formaggio, A. Barazza, A. Bertocco, C. Toniolo, Q. B. Broxterman, B. Kaptein, E. Brasola, P. Pengo, L. Pasquato and P. Scrimin, *J. Org. Chem.*, 2004, **69**, 3849–3856; (*c*) Y. Kosugi, M. Akakura and K. Ishihara, *Tetrahedron*, 2007, **63**, 6191–6202; (*d*) X.-L. Geng, J. Wang, G.-X. Li, P. Chen, S.-F. Tian and J. Qu, *J. Org. Chem.*, 2008, **73**, 8558–8562.

18 (*a*) S. Tabanella, I. Valancogne and R. F. W. Jackson, *Org. Biomol. Chem.*, 2003, **1**, 4254–4261; (*b*) H. Schedel, K. Kan, Y. Ueda, K. Mishiro, K. Yoshida, T. Furuta and T. Kawabata, *Beilstein J. Org. Chem.*, 2012, **8**, 1778–1787.

19 (*a*) T. Kawabata, R. Stragies, T. Fukaya, Y. Nagaoka, H. Schedel and K. Fuji, *Tetrahedron Lett.*, 2003, **44**, 1545–1548; (*b*) G. Priem, B. Pelotier, S. J. F. Macdonald, M. S. Anson and I. B. Campbell, *J. Org. Chem.*, 2003, **68**, 3844–3848; (*c*) B. Pelotier, G. Priem, S. J. F. Campbell, M. S. Anson, R. J. Upton and I. B. Campbell, *Tetrahedron Lett.*, 2005, **46**, 9005–9007; (*d*) Y. Ueda, W. Muramatsu, K. Mishiro, T. Furuta and T. Kawabata, *J. Org. Chem.*, 2009, **74**, 8802–8805; (*e*) H. Mandai, S. Irie, M. Akehi, K. Yuri, M. Yoden, K. Mitsudo and S. Suga, *Heterocycles*, 2013, **87**, 329–340.

20 (*a*) Y. Wei, L. Held and H. Zipse, *Org. Biomol. Chem.*, 2006, **4**, 4223–4230; (*b*) L. Mesas-Sanchez and P. Diner, *Chem. – Eur. J.*, 2015, **21**, 5623–5631.

21 H. B. Kagan and J. C. Fiaud, *Top. Stereochem.*, 1988, **18**, 249–330.

22 N. M. O'Boyle, M. Banck, C. A. James, C. Morley, T. Vandermeersch and G. R. Hutchison, *J. Cheminform.*, 2011, **3**, 1–14.

23 T. A. Halgren, *J. Comput. Chem.*, 1996, **17**, 490–519.

24 R. Sure and S. Grimme, *J. Comput. Chem.*, 2013, **34**, 1672–1685.

25 A. D. Becke, *J. Chem. Phys.*, 1993, **98**, 5648.

26 C. Lee, W. Yang and R. G. Parr, *Phys. Rev. B: Condens. Matter*, 1988, **37**, 785–789.

27 S. H. Vosko, L. Wilk and M. Nusair, *Can. J. Phys.*, 1980, **58**, 1200–1211.

28 F. Weigend and R. Ahlrichs, *Phys. Chem. Chem. Phys.*, 2005, **7**, 3297–3305.

29 S. Grimme, J. Antony, S. Ehrlich and H. Krieg, *J. Chem. Phys.*, 2010, **132**, 154104.

30 S. Grimme, S. Ehrlich and L. Goerigk, *J. Comput. Chem.*, 2011, **32**, 1456–1465.

31 F. Neese, *J. Comput. Chem.*, 2003, **24**, 1740–1747.

32 F. Neese, F. Wennmohs, A. Hansen and U. Becker, *Chem. Phys.*, 2009, **356**, 98–109.

33 S. Sinnecker, A. Rajendran, A. Klamt, M. Diedenhofen and F. Neese, *J. Phys. Chem. A*, 2006, **110**, 2235–2245.

34 F. Neese, *WIREs Comput. Mol. Sci.*, 2012, **2**, 73–78.

35 (*a*) C. Janiak, *J. Chem. Soc., Dalton Trans.*, 2000, 3885–3896; (*b*) C. R. Martinez and B. L. Iverson, *Chem. Sci.*, 2012, **3**, 2191–2201.

36 J. Řezáč, K. E. Riley and P. Hobza, *J. Chem. Theor. Comput.*, 2011, **7**, 2427–2438.

37 X. Li, P. Liu, K. N. Houk and V. Birman, *J. Am. Chem. Soc.*, 2008, **130**, 13836–13837.

38 C. B. Shinisha and R. B. Sunoj, *Org. Lett.*, 2009, **11**, 3242–3245.

39 (*a*) N. De Rycke, G. Berionni, F. Couty, H. Mayr, R. Goumont and O. R. P. David, *Org. Lett.*, 2011, **13**, 530–533; (*b*) T. Poisson, S. Oudeyer and V. Levacher, *Tetrahedron Lett.*, 2012, **53**, 3284–3287.

